

Research and Innovation action

NUMBER — 955387 — LEON-T

# LEON-T

*Low particle Emissions and IOw Noise Tyres*



Deliverable No.	3.4	
Deliverable Title	Updated emission model for local and EU scale	
Dissemination	PU	
Written by	J. Meesters, J.T.K. Quik (RIVM)	16/06/2023
Checked by	Anna Schwarz (TNO)	23/06/2023
Approved by	Juan Garcia (IDIADA)	03/07/2023
Issue date	05/07/2023	



This Project has received funding from the European Union's Horizon 2020 research and innovation programme under grant agreement N° 955397. The content of this report reflects only the author's view CINEA is not responsible for any use that may be made of the information it contains.

## Revision history

REVISION	DATE	DESCRIPTION	AUTHOR (ORGANIZATION)
0	16 June 2023	First complete version of the deliverable	Joris Meesters (RIVM)
1	21 June 2023	Review by project/WP partner	Anna Schwarz (TNO)
2	29 June 2023	Internally approved	Theo Traas (RIVM)
3	3 July 2023	Final approved version by LEON-T coordinator	Juan J García
4	18 nov. 2024	Update with IDIADA track data	Joris Meesters (RIVM)

## Content

<b>1</b>	<b>INTRODUCTION</b>	<b>6</b>
1.1	Nano and microplastics	6
1.2	Tyre wear release	6
1.3	Tyre wear abrasion coefficient	7
1.4	Aim	8
<b>2</b>	<b>METHODS</b>	<b>9</b>
2.1	Model concept	9
2.1.1	Background	9
2.1.2	Wheelspin slip simulation	12
2.1.3	Simulation of slip during brake manoeuvres	13
2.1.4	Latitudinal slip simulation	13
2.2	Deriving abrasion coefficients	13
2.3	Model input	14
2.4	Friction model evaluation	15
2.4.1	Uncertainty and sensitivity analysis	15
2.4.2	Illustrative case studies	16
2.5	Availability	17
<b>3</b>	<b>RESULTS</b>	<b>18</b>
3.1	Sensitivity analysis	18
3.2	Estimated abrasion coefficients	20
3.2.1	IDIADA tyre wear comparison	21
3.2.2	ADAC track derived abrasion coefficients	21
<b>4</b>	<b>DISCUSSION</b>	<b>21</b>
4.1	Model evaluation	21
4.1.1	Opportunities for model validation	22
4.1.2	Calibration of peak friction coefficient and optimal slip	23
4.1.3	The importance of abrasion coefficient	23
4.2	Perspective	24
4.2.1	Adapting emission factors	24
4.2.2	Predicting impact of policy measures	24
<b>5</b>	<b>CONCLUSION</b>	<b>24</b>

<b>6</b>	<b>REFERENCES</b>	<b>25</b>
<b>7</b>	<b>APPENDIX</b>	<b>28</b>
<b>7.1</b>	<b>Sensitivity analysis</b>	<b>28</b>
7.1.1	Additional sensitivity rankings	28
<b>7.2</b>	<b>ADAC Track sector data</b>	<b>30</b>
<b>8</b>	<b>APPENDIX II CIRCUIT RUN DATA</b>	<b>30</b>
<b>8.1</b>	<b>Vehicle specifications</b>	<b>30</b>
<b>8.2</b>	<b>Tyre quality and design</b>	<b>31</b>
<b>8.3</b>	<b>IDIADA track and maneuver data</b>	<b>32</b>
8.3.1	Oval track	32
8.3.2	Urban Loop	33
8.3.3	Urban parking	35
<b>8.4</b>	<b>Performed maneuvers</b>	<b>36</b>
8.4.1	Run-in procedure	36
8.4.2	Rural driving	37
8.4.3	Motorway	41
8.4.4	Urban driving	42

# 1 Introduction

## 1.1 Nano and microplastics

The release of nano and microplastics (NMPS) into the environment is of increasing concern as a growing volume of microplastics is found in the environment, including the sea, food, drinking water, plant life and terrestrial ecosystems. Once in the environment, microplastics degrade very poorly and slowly, so that they tend to accumulate. Moreover, NMPs are able to reach pristine environments such mountain tops, polar regions, and ocean water as they disperse through the atmosphere, troposphere, surface water bodies and groundwater (Schwarz et al., 2023; Zhang et al., 2020). Environmental pollution with plastics will keep on increasing if no measures against their release and presence in the environment are taken (Lau et al., 2020). Tackling plastic pollution as such is a challenge, not to be taken lightly (Borrelle et al., 2020). Specifically reducing the unintentional release of NMPs to the environment requires additional effort. This is part of the European Green Deal and circular economy action plan, but at the moment has not yet resulted in a concrete proposal of policy measures , see [Microplastics \(europa.eu\)](https://ec.europa.eu/euro-observatory/en/microplastics).

## 1.2 Tyre wear release

The release of tyre wear particles (TWPs) is considered to be a major source of microplastic release, but the level of uncertainty in the estimated quantities is great. Recent studies use nationally derived (Ntziachristos and Boulter, 2019), country specific, emission factors (EFs) to quantify TWP emissions per year per country (Mennekes and Nowack, 2022). EFs are defined as the mass TWP released per driven distance, often expressed in mg/km. The EFs can be differentiated per vehicle class, such as passenger cars, light and heavy duty vehicles, motor cycles and the location and type road such as highways, urban streets and rural motorways (Ntziachristos and Boulter, 2019; Verschoor et al., 2014). However, a recent analysis on the data underpinning the EFs derived for 14 different countries demonstrates a great level of uncertainty (Mennekes and Nowack, 2022). The EF data are often taken from publications that do not directly present own measurement data of tyre wear per kilometre driven under different circumstances with different vehicles. Instead EFs are cited from publications that present EFs cited from earlier publications. The result is that EFs are derived from a network of 63 studies that include only three trustful sources of measurement data, but these are cited only three times within the EF publication network (Mennekes and Nowack, 2022). The remaining underpinning data could not be found, or refer to outdated measurements performed in the 1970's. As such, the EFs are uncertain and do not sufficiently cover innovations in vehicle design and tyre quality achieved by the automotive industry and tyre branch over the last decades, whereas part of the approach of the European Commission (EC) is to encourage innovations of the market (Directorate-General for Research and Innovation (European Commission) and Groupe des conseillers scientifiques principaux, 2019) .

Therefore, there is a need for emission factors that better represent the current tyre, automotive and road technology in use. Furthermore, for driving and evaluating mitigating measures there is a need for including more variables than the commonly used vehicle and road type in combination with vehicle speed for determining overall tyre wear related emissions. An important aspect relevant for the emission factor is the tyre itself, but also behavioural aspects and the landscape characteristics are known factors influencing tyre wear (Ejsmont et al., 2014, 2012; Gehrke et al., 2020; Kühlwein, 2016). These factors can be understood by looking at the physical forces affecting tyre wear formation.

### 1.3 Tyre wear abrasion coefficient

The physical forces affecting tyre wear can be quantified using model equations which in turn then can be used to estimate the release of NMPs due to tyre wear. The model equations predict the amount of tyre wear released as a function of vehicle specifications, tyre quality, driving manoeuvres and characteristics of the landscape and road. These were already derived several decades ago (Schallamach and Turner, 1960). The model equations as derived by Schallamach and Turner (1960) and included in their, relatively simple, wear model still form the basis for studies on vehicle performance, safety and innovations (Cunha et al., 2007; Da Silva et al., 2012; Grip, 2021; Pohrt, 2019) as well as recent environmental modelling studies on TWP release (Fraunhofer et al., 2021; Gehrke et al., 2020; Steiner, 2020). These models describe that the quantity of tyre wear (mg) as proportional to the friction work (J) performed at the interface between tyre and track. The friction work is calculated as the sum of the resistive forces (N) performed on the tyres in longitudinal and latitudinal directions multiplied with distance (m) and slip (which is defined as the relative difference between vehicle velocity and radiant velocity of the wheels). The proportionality between the friction work and tyre wear is expressed as an abrasion coefficient (mg/J), see equation 1.

$$\text{wear (mg)} = \text{abrasion coefficient (mg/J)} \times \text{friction work (J)} \quad (\text{Eq 1})$$

The abrasion coefficient is considered to be a property of the tyre that is independent of landscape or vehicle characteristics. Often, measurement data on the abrasion coefficient of tyres is not available and is therefore treated as an uncertain or unquantified tyre quality parameter (Fraunhofer et al., 2021; Gehrke et al., 2020; Pohrt, 2019). Taking into account the linear relationship between wear and the abrasion coefficient allowed the spatial modelling studies (Gehrke, 2020; Fraunhofer et al., 2021) on TWP release to identify local hotspots (see Figure 1). However, these models are in dire need of high quality abrasion coefficients to reduce the uncertainty in their absolute estimates of release of tyre wear. Furthermore, fixed values of slip were applied for the different manoeuvres such as accelerating, braking and cornering. Inclusion of an algorithm describing the relationship between slip and performed vehicle manoeuvres are needed in order to better estimate the influences of driver behaviour, vehicle design, tyre design and local road

characteristics. This is particularly relevant when considering the reduction potential of different mitigation measures.

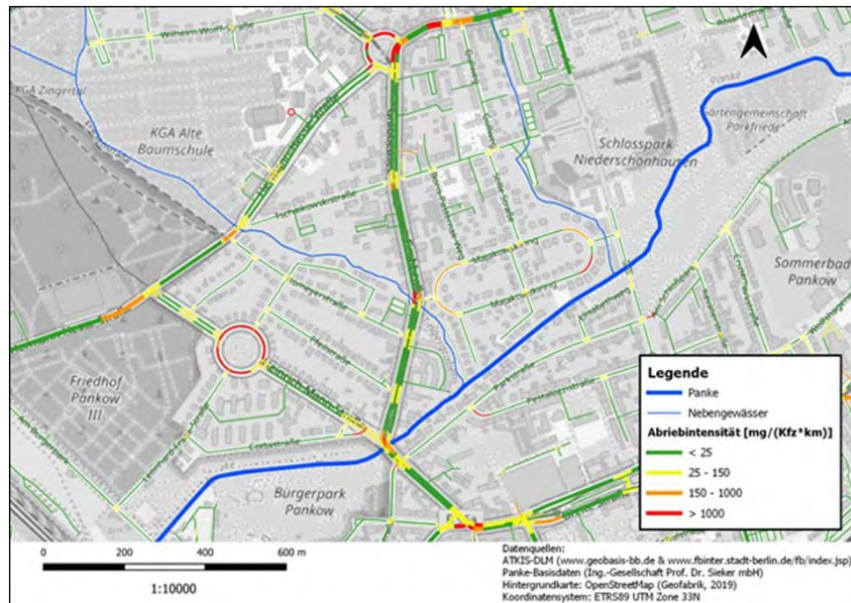


Figure 1: TyreWearMap estimated abrasion intensity in a local area near the Panke river using a modelling approach that includes the relationship between wear, friction work and the abrasion coefficient (equation 1). Figure from German TyreWearMap report (Fraunhofer et al., 2021).

## 1.4 Aim

This report consists of two major goals:

1. Provide an approach for estimation of abrasion coefficients of tyres based on standardised abrasion measurements using the relationship between wear, friction work and the abrasion coefficient. These abrasion data are or will become available from driving a passenger car over a track circuit with different tyres (LEON-T D2.1), indoor laboratory measurements of tyre abrasion (Leon-T D2.3) and tyre abrasion rates (mg/km) from abrasion tests with known driven routes from the IDIADA test track.
2. Present a tyre friction and abrasion model that can be used to estimate TWP release for different vehicles, tyres, landscapes and roads .

In this deliverable, we present an adaption and extension of previously published models (Gehrke, 2020; Pohr, 2019; Fraunhofer Institute, 2021) to estimate abrasion coefficients of tyre sets currently available on the consumer market. These abrasion coefficients can then be used to derive updated EFs, so that the existing modelling approaches can be easily applied to get improved environmental release estimates. The model simulations of abrasion of different tyres also allows for validation with field measurements performed at different traffic situations and local landscapes (Leon-T D3.2). Such model validation efforts should eventually provide for a robust modelling approach to estimate tyre wear release considering different vehicles, tyres, driving manoeuvres, local roads and local



landscapes. As such, the impact of mitigating measures related to vehicle innovations can be quantified, such as improved aerodynamics, tyre innovations, such as reduced tyre roll resistance for saving fuel consumption, or other system changes such as adapting speed limits or reducing traffic congestion.

## 2 Methods

### 2.1 Model concept

#### 2.1.1 Background

The basic concept of predicting tyre wear from vehicle manoeuvres is based on Schallamach and Turners wear model (Schallamach and Turner, 1960) which is a relative simple model that is commonly used in tyre wear and performance simulations (Cunha et al., 2007; Da Silva et al., 2012; Fraunhofer Institute, 2021; Gehrke et al., 2020; Grip 2021; Pohrt, 2019). The wear quantity is estimated with an abrasion coefficient which is a constant that expresses the abraded mass per unit of dissipation energy ( $\text{mg}\cdot\text{J}^{-1}$ ) multiplied with the friction work performed (Equation 1). The friction work is calculated per manoeuvre a vehicle is anticipated to perform in a sector which are acceleration, deceleration, driving at constant speed and cornering. Per manoeuvre, the friction work is calculated as the product of:

- i. the sum of all resistive forces acting on the vehicle in longitudinal and latitudinal direction in *Newton (N)*
- ii. the slip ratio which refers to the difference between the actual vehicle velocity and the wheel angular velocity of the wheels multiplied with the wheel radius in  $(\text{m}\cdot\text{s}^{-1})/(\text{m}\cdot\text{s}^{-1})$  (-)
- iii. the distance covered in *meters (m)*.

Per type manoeuvre it is determined which longitudinal and latitudinal forces act on the tyres, what type of slip the tyre is subjected to and over what distance the manoeuvre is performed (Table 1).

Table 1: Calculation of longitudinal resistive forces, slip and distance per vehicle manoeuvre

Maneuver	Distance (m)	Slope grade (%)	Additional braking needed	Longitudinal resistive forces	Slip
Acceleration	$S = vt + \frac{1}{2}at^2$ $t = \frac{v_t - v_0}{c_{accel}}$	Flat (0%)	No	$F_{roll} + F_{drag} + F_{inert}$	Wheel spin
		Uphill (>0.%)	No	$F_{roll} + F_{drag} + F_{inert} + F_{slope}$	Wheel spin
		Downhill (<0%)	No	$F_{roll} + F_{drag} + F_{inert}$	Wheel spin
Constant speed	$S_{sector} - S_{accel} - S_{decel}$	Flat (0%)	No	$F_{roll} + F_{drag}$	Wheel spin
		Uphill (>0.%)	No	$F_{roll} + F_{drag} + F_{slope}$	Wheel spin
		Downhill (<0%)	No <sup>*A</sup> , if $ F_{slope}  <  F_{roll} + F_{drag} $	$F_{roll} + F_{drag}$	Wheel spin
			Yes <sup>*B</sup> , $ F_{slope}  > (F_{roll} + F_{drag})$	$F_{roll} + F_{drag} + F_{brake}$ , with $F_{brake} =  F_{slope}  - (F_{roll} + F_{drag})$	Brake
Deceleration	$S = vt + \frac{1}{2}dt^2$ $t = \frac{v_0 - v_t}{c_{decel}}$	Flat (0%)	No <sup>*C</sup> if $c_{decel} < c_{decel, resist}$	$F_{roll} + F_{drag}$	Wheel spin
			Yes <sup>*D</sup> , if $c_{decel} > c_{decel, resist}$	$F_{roll} + F_{drag} + F_{brake}$ , with $F_{brake} =  (m_{vehicle} + m_{rot, parts}) \times c_{decel}  - (F_{roll} + F_{drag})$	Brake
		Uphill (>0.%)	No <sup>*E</sup> if $c_{decel} < c_{decel, resist}$	$F_{roll} + F_{drag} + F_{slope}$	Wheel spin
			Yes <sup>*F</sup> , if $c_{decel} > c_{decel, resist}$	$F_{brake} =  (m_{vehicle} + m_{rot, parts}) \times c_{decel}  - (F_{roll} + F_{drag} + F_{slope})$	Brake
		Downhill (<0%)	No <sup>*G</sup> if $c_{decel} < c_{decel, resist}$	$F_{roll} + F_{drag}$	Wheel spin
			Yes <sup>*H</sup> if $c_{decel} > c_{decel, resist}$	$F_{roll} + F_{drag} + F_{brake}$ , with $F_{brake} =  (m_{vehicle} + m_{rot, parts}) \times c_{decel}  - (F_{roll} + F_{drag} -  F_{slope} )$	Brake

A: Additional brake force is not needed to remain under the speed limit if the resistive drag and roll forces are larger than the downhill slope force, i.e. laying the foot of the gas is sufficient to keep the vehicle down under speed limit.

B: additional brake force is needed to remain under speed limit, because the downhill slope is so steep that the vehicle is powered by the downhill slope force is greater than the resistive roll and drag force

C: the deceleration caused by the roll and drag force  $(c_{decel, resist}) = (F_{roll} + F_{drag}) / (m_{vehicle} + m_{rot, parts})$  sufficiently slows the vehicle down for a desired deceleration rate constant ( $c_{decel}$ ), i.e. laying the foot of the gas is sufficient to slow the vehicle down

D: additional brake force is needed, because drag and roll resistance are not great enough to slow the vehicle down with the desired deceleration constant.

E: brake force is not needed because, drag, roll and uphill slope force sufficiently slow the vehicle down.

F: additional brake force is needed, because the drag, roll and uphill slope resistance are not great enough to reach the desired deceleration constant.

G: drag and roll force sufficiently slow the vehicle down once the driver lays the foot of the gas despite the downhill slope force powering the vehicle.

H: additional brake force is needed as the drag and roll resistance are not great enough to reach the desired deceleration constant as the vehicle is also powered by the downhill slope force.

The longitudinal forces acting on a vehicle are the roll resistance force at the interface of track and tyre, the aerodynamic drag force, slope force upon uphill driving, inertia force upon acceleration, and brake force if needed to decelerate or to maintain a speed limit at downhill driving, whereas the latitudinal resistant forces considered are the centripetal and bank slope force during a corner manoeuvre (Wilde, 2012; 2014; Pohrt, 2019). Slip is defined as the difference between the actual vehicle velocity and the radiant velocity of the wheels (Figure 2). The model presented in this deliverable report includes two type of slip activities which are: (i) wheelspin: the wheel velocity is faster than the forward velocity of the vehicle but slips due to a lack of traction and (ii) braking: vehicle is still moving in forward direction but a brake force limits the wheel velocity.

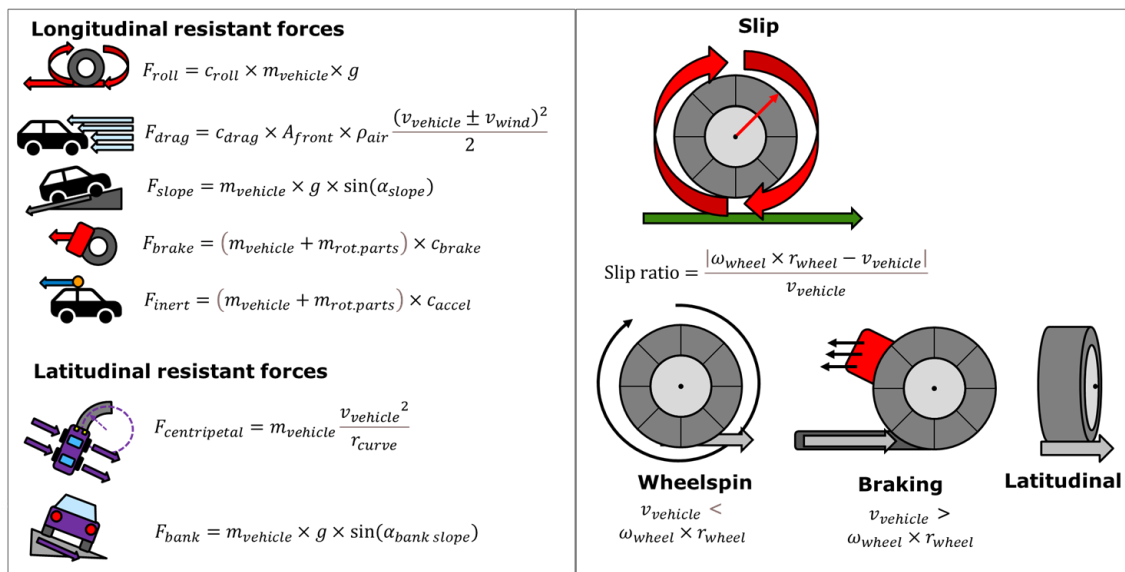


Figure 2: Overview of model routines for simulating longitudinal and latitudinal forces with longitudinal roll force ( $F_{roll}$ ), aerodynamic drag force ( $F_{drag}$ ), slope force ( $F_{slope}$ ), brake force ( $F_{brake}$ ), inertia force upon accelerating ( $F_{inert}$ ) and the latitudinal centripetal force ( $F_{centripetal}$ ) and bank force ( $F_{bank}$ ) in N based on the tyre's roll coefficient ( $c_{roll}$ ) in kg/kg, the mass of the vehicle ( $m_{vehicle}$ ) in kg, the drag coefficient of the vehicle ( $c_{drag}$ ) (unitless), the mass of the rotating parts of the vehicle ( $m_{rot,parts}$ ) in kg, the slope of the road in longitudinal direction ( $\alpha_{slope}$ ) in ° and bank slope of the road in latitudinal direction ( $\alpha_{bankslope}$ ) in °, radius of the curve upon cornering ( $r_{curve}$ ) in m, velocity of the driving maneuver ( $v_{vehicle}$ ) in  $m.s^{-1}$ , acceleration constant ( $c_{accel}$ ) in  $m.s^{-2}$  and braking ( $c_{brake}$ ) in  $m.s^{-2}$ , density of air ( $\rho_{air}$ ) in  $kg.m^{-3}$ , wind speed ( $v_{wind}$ ) in  $m.s^{-1}$  and the gravitational acceleration constant ( $g$ ) in  $m.s^{-2}$ ,  $\omega_{wheel}$  is the wheel angular velocity of the wheel in  $rad.s^{-1}$ ,  $r_{wheel}$  is the radius of the wheel in m.

## 2.1.2 Wheelspin slip simulation

The vehicle manoeuvres acceleration, constant speed driving and deceleration are assumed to be performed in the low slip regime (Pohrt, 2019), so that wheelspin slip is linear to the friction coefficient between tyre and track (Figure 3).

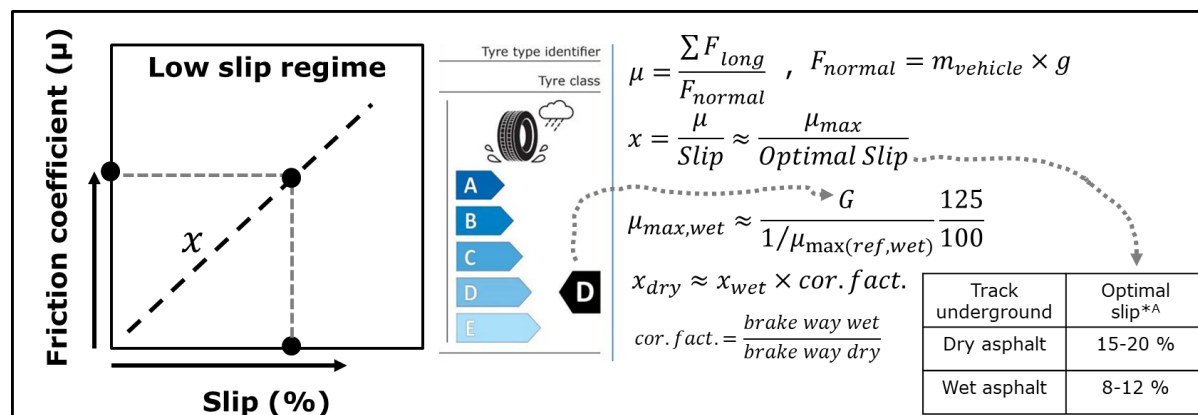
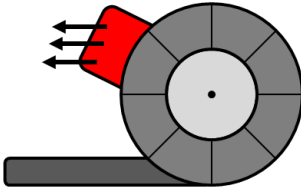


Figure 3: Calculation of the Friction coefficient based on tyre grip index score (G).

The friction coefficient is calculated as the sum of the longitudinal resistive forces ( $\sum F_{long}$ ) divided by the downward normal force ( $F_{normal}$ ). The linearity ( $x$ ) between friction coefficient and slip is approached as the ratio of the peak friction coefficient and the optimal slip ratio between tyre and track. The peak friction coefficient is estimated from the tyre's wet grip index (see appendix 7.2 Table 2) which producers must indicated with the EU2020/740 consumer label (EU, 2020). As such grip index scores (G) are publicly available in the European Product Registry for Energy Labelling (EPREL) database for each type of tyre available on the EU consumer market after the introduction of the new label ([EPREL Public website \(europa.eu\)](https://eprel.ec.europa.eu/)). The wet grip index actually refers to how a measured peak friction coefficient of the tyre on wet asphalt relates to the peak friction coefficient of a reference tyre. The EC describes a test procedure in which a passenger car brakes with maximal effort to decelerate from 80 to 20 km/h on a wet asphalt track in the EU regulation 228/2011 (EC, 2011). The grip index is then scored according to measured distance of the deceleration manoeuvre compared with a reference distance. Here, the relationship between tyre grip index and peak friction coefficient is simplified by assuming the conditions at which the peak friction coefficient was measured are equal to the reference conditions described in the EC test procedure (EC, 2011) to derive wet grip indexes. The peak friction coefficient of the EC reference tyre at EC reference conditions is 0.85, so that the peak friction coefficient between tyre and track can be approached under wet conditions if the EU grip index label is available. Next, the linearity is corrected from wet to dry conditions by the ratios of brake way distances under both conditions. Based on tyre brake test under wet and dry conditions (AutoBild, 2021) this correction factor is estimated to be 1.07 – 1.47.

### 2.1.3 Simulation of slip during brake manoeuvres

The slip ratio during brake manoeuvres is calculated as the ratio of the deceleration constant yielded by the (additional) brake force exerted during the manoeuvre ( $C_{brake.manoeuvre}$ ) to the deceleration constant of the tyre at a full wheel lock ( $C_{full.brake}$ ). The full brake deceleration constant is proportional to the tyre's grip index and peak friction coefficient (EC, 2011). The reference deceleration constant of a reference tyre under reference wet conditions is 0.68 g (6.8 m.s<sup>-2</sup>) (EC, 2011). Next, the full brake deceleration constant on wet asphalt is then corrected to dry conditions with the dry to wet correction factor.



$$C_{brake.manoeuvre} = \frac{F_{brake.manoeuvre}}{m_{vehicle} + m_{rot.part.s} G} \frac{125}{100}$$

$$C_{full.brake.wet} \approx \frac{1}{C_{full.brake(ref,wet)}} \frac{125}{100}$$

$$C_{full.brake.dry} \approx cor. fact \times C_{full.brake.wet}$$

$$Slip \approx \frac{C_{brake.manoeuvre}}{C_{full.brake}}$$

Figure 4: Slip during braking manoeuvre

### 2.1.4 Latitudinal slip simulation

Tyre abrasion by latitudinal forces is about 7 times more effective than by longitudinal forces, which means the product of lateral abrasion coefficient and lateral slip is about 7 times greater than the product of longitudinal abrasion coefficient and longitudinal slip (Pohrt, 2019). In order to derive one single value for the abrasion coefficient the lateral slip is estimated a factor 7 greater than longitudinal slip. This factor is included in the calculation of the linearity between friction coefficient and slip (Equation 2).

$$\mu_{lat} = \frac{\sum F_{lat}}{F_{normal}}, x_{lat} \sim \frac{\mu_{lat}}{7 \times slip} \quad \text{Eq. 2}$$

## 2.2 Deriving abrasion coefficients

The abrasion coefficient data of tyres is often not directly available, since abrasion of tires is often expressed as an abrasion rate (mg/km) that reflects the tire mass abraded per driven kilometre (mg/km). Tire abrasion coefficients (mg/J) are therefore derived from datasets in literature that describe the driven track, the test vehicle used, the tires mounted on the vehicle and the measured abrasion rates (mg/km), Equation 3. The characteristics of the track and test vehicle are then inserted as input values in the model

to calculate the total longitudinal and latitudinal friction work performed on the tires over the distance (km) of the entire test track.

$$\text{abrasion coefficient} = \frac{\text{abrasion rate}}{(\text{long.} + \text{lat. Friction Work}) / \text{track distance}} \quad \text{Eq. 3.}$$

## 2.3 Model input

The input data required to simulate the model routines are

- (i) vehicle specifications, such as vehicle mass, the mass of the rotating parts of the vehicle, frontal area, drag coefficient and the 0-100 km/h acceleration time
- (ii) tyre quality and design, such as grip index and roll resistance coefficient
- (iii) track characteristics, such as slope, road texture and wet or dry conditions
- (iv) driving style and manoeuvres

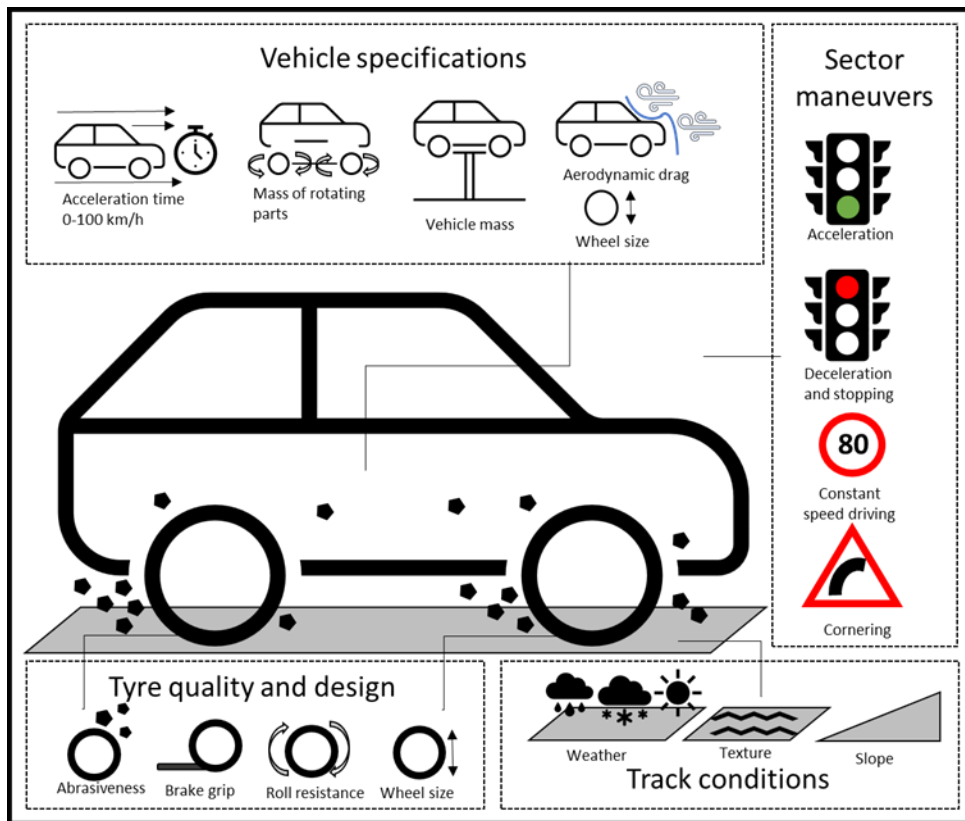


Figure 5. Visualization of TWP emission model input

## 2.4 Friction model evaluation

### 2.4.1 Uncertainty and sensitivity analysis

A global sensitivity analysis is performed to understand whether the model functions as expected in predicting the amount friction work performed on the tyres for different manoeuvres and variable values representing vehicle specification, driving style, tyre quality and local road and landscape characteristics (Table 2). This is done with a Monte Carlo analysis of the friction work as calculated based on the relevant parameter space for each variable ( $n=10,000$ ). The analysis was done for the friction work as total and for the friction work per distance, as the friction work per distance is needed to calculate the abrasion coefficient based on the measured abrasion (see equation 1). The min and max for each two variables are used in a uniform distribution to estimate the uncertainty and variability of the resultant friction work (see Table 2).

Next, the moment independent sensitivity importance measures are calculated using the method proposed by Borgonovo (Borgonovo, 2007; Plischke and Borgonovo, 2020). These were used to rank all (uncertain and variable) parameters in terms of their contribution to uncertainty in the resulting friction work. The analysis is performed for each manoeuvre separately and for a case where 10,000 m is combined using 1 section for each manoeuvre. We calculated these sensitivity measures using the *sensiFdiv function* in the *sensitivity package for R* (R Core Team, 2023) developed by looss et al. (2023).

Table 2: Variable input distributions used in Monte Carlo simulations, including the relevant constants.

	Description	Variable name	Min	Max
<b>Vehicle specifications</b>	Vehicle mass in kg	m_vehicle	900	2000
	Vehicle frontal area in $m^2$	A_vehicle	2	3
	Vehicle aerodynamic drag coefficient	c_drag_vehicle	0.2	0.4
	Vehicle acceleration time reaching 0-100 kmh in s	t_0_100kmh_vehicle	8	20
	The fraction of the mass of the vehicle consisting of rotating parts in kg/kg	frac_mass_rotate_parts_vehicle	0.13	0.15
	Vehicle turning diameter	d_turn_vehicle	9.8	9.8
<b>Tyre quality</b>	Tyre grip (G) index (EU label 2020)	grip_index_tyre	1.09	1.55
	Tyre roll coefficient (EU label 2020)	c_roll_tyre	6.5	10.6
<b>Track underground dry</b>	Optimal slip	Optimal_slip_track	0.15	0.2

<b>Track underground wet</b>	Optimal slip	Optimal_slip_track	0.08	0.12
<b>Track underground dry</b>	Correction factor for "wet" to "dry" conditions	x_correct_track	1.07	1.47
<b>Track underground wet</b>	Correction factor for "wet" to " wet" conditions	x_correct_track	1	1
<b>Track underground</b>	Peak friction coefficient of EU reference tyre on EU reference track	mu_max_ref_tyre	0.85	0.85
<b>Track underground</b>	Brake deceleration constant of EU reference tyre on EU reference track in g	c_full_brake_ref_tyre	0.68	0.68
<b>Sector</b>	Sector distance in m	sector_distance	10000	10000
	Vehicle velocity at start of sector in km/h	sector_start_velocity_kmh	0	80
	Vehicle velocity at middle of sector in km/h	sector_velocity_kmh	80	140
	Vehicle velocity at end of sector in km/h	sector_end_velocity_kmh	0	80
	Slope angle (%)	alpha_slope	-10	10
	Radius of corner in sector in m	sector_corner_radius	0	800
	Corner angle of sector in degree	sector_corner_angle	0	360
	Bank slope of corner in sector (%)	sector_bank_slope	-10	10
	<b>Environmental conditions and physics</b>	Gravitational acceleration constant m.s-2	grav_constant	9.81
Wind speed in ms.-1		v_wind	-5	5
Density of air (kg/m3)		rho_air	1.205	1.205
<b>Behavior</b>	Comfortable deceleration constant	c_decel_comfort	2	3
		frac_driver_comfort_max_accelaration	0.1	1

### 2.4.2 IDIADA track simulations

Within work package 2 of the LEON-T project, measurements on tyre abrasion have been performed on the IDIADA track (Figure 7). The vehicle specifications of the passenger car (Ford Kuga Escape) that drove the track are available as well as the driving style parameters, such as velocity, deceleration and acceleration constant. The driving manoeuvres performed during the tyre wear measurements at the IDIADA track have



been simulated with the friction model in order to derive the abrasion coefficients of the different tyre sets mounted on the vehicle and to express wear rates projected per vehicle manoeuvre. Abrasion coefficients (mg/J) are derived by dividing measured abrasion rate (mg/km) with the simulated level of friction work performed per kilometre (J/km). The necessary data, such as the specifications of the vehicle, the tyres mounted on the vehicle, the route or track that was driven, and the measured abrasion rates (mg/km) per tyre from driving the track are described in detail in Appendix II. Five circuit runs have been performed for each tyre abrasion test scenario representing rural, urban and motorway driving (Appendix II).

## 2.5 Availability

The model code is made available under the EUPL-1.2 license: <https://github.com/rivm-syso/tyre-friction-abrassion-emission>.

### 3 Results

#### 3.1 Sensitivity analysis

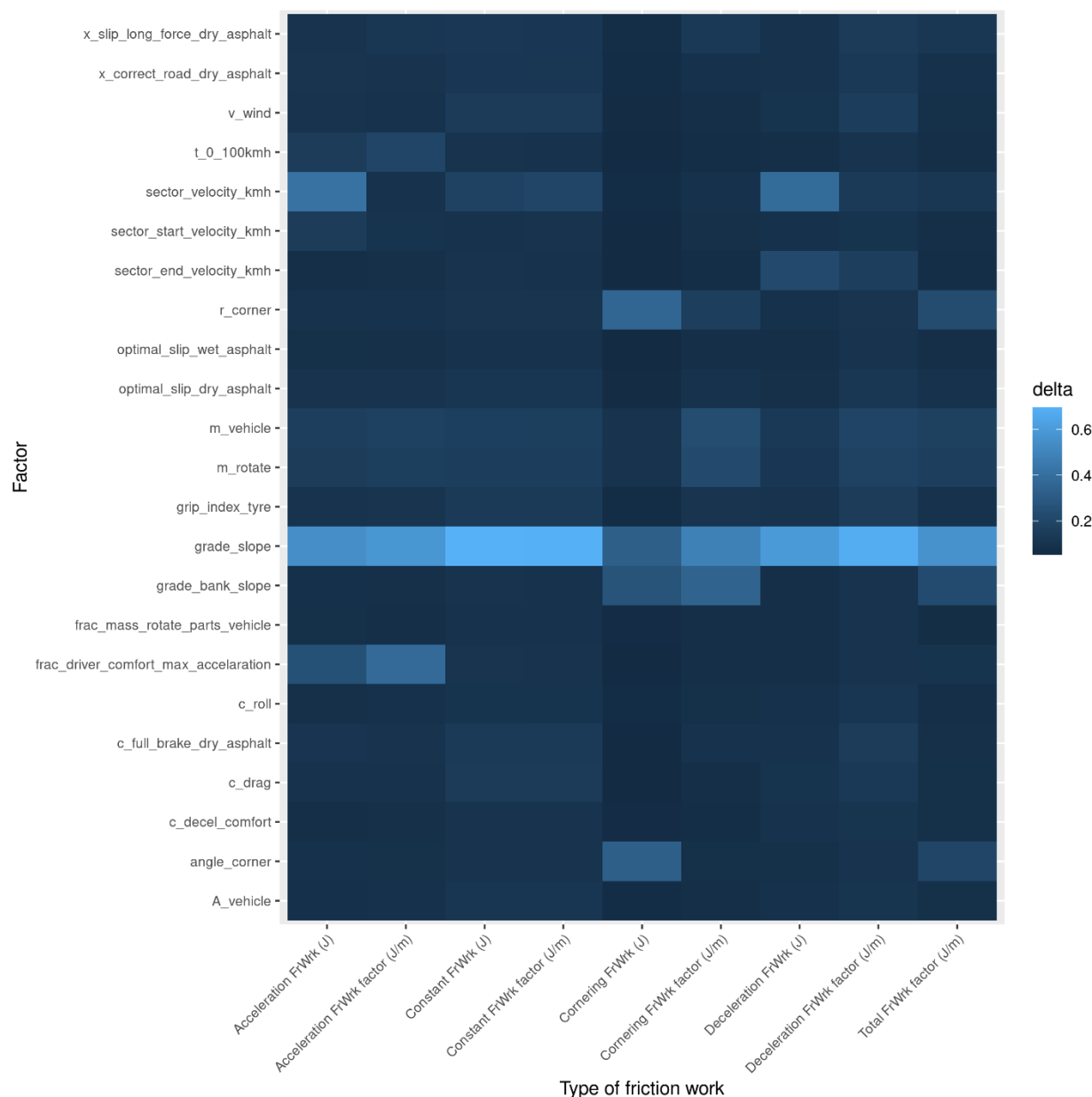


Figure 5: Sensitivity ranking of model parameters as described in Table 2.

A global sensitivity analysis was conducted to determine sensitivity rankings for 21 uncertain and variable model inputs (Figure 5). The slope of the road is the most sensitive variable, both for the Total friction work per distance and the subset of friction work absolute and per distance for the separate manoeuvres. Other less sensitive variables are the bank slope and corner radius and angle. Slope is found to be an important factor in tyre wear, but the variability inserted in the analysis refer to a mountain landscape where slope grades may differ from -10 to 10 %. The sensitivity of the friction model

outcomes to slope is so strong that it obscures the sensitivity to other input parameters (Figure 5 and 6). For example, slope still has the highest relative sensitivity ranking even at a 10 times smaller input range (-1 to 1%, see Figure 8 and in Appendix 7.1.1).

Given this sensitivity of the model to the slope of the road, we now consider a scenario where the road is flat (slope is 0 and not varying anymore, Figure 6). Where in the previous analysis slope was most sensitive, it is now the bank slope. Bank slope however is included in the simulation of corner manoeuvres. The model for the total friction work is also sensitive to the other parameter describing the corner, such as the angle and radius. Although the scenario here is not representative of real driving conditions it is clear that variation in cornering will have a large effect on determining the abrasion coefficient.

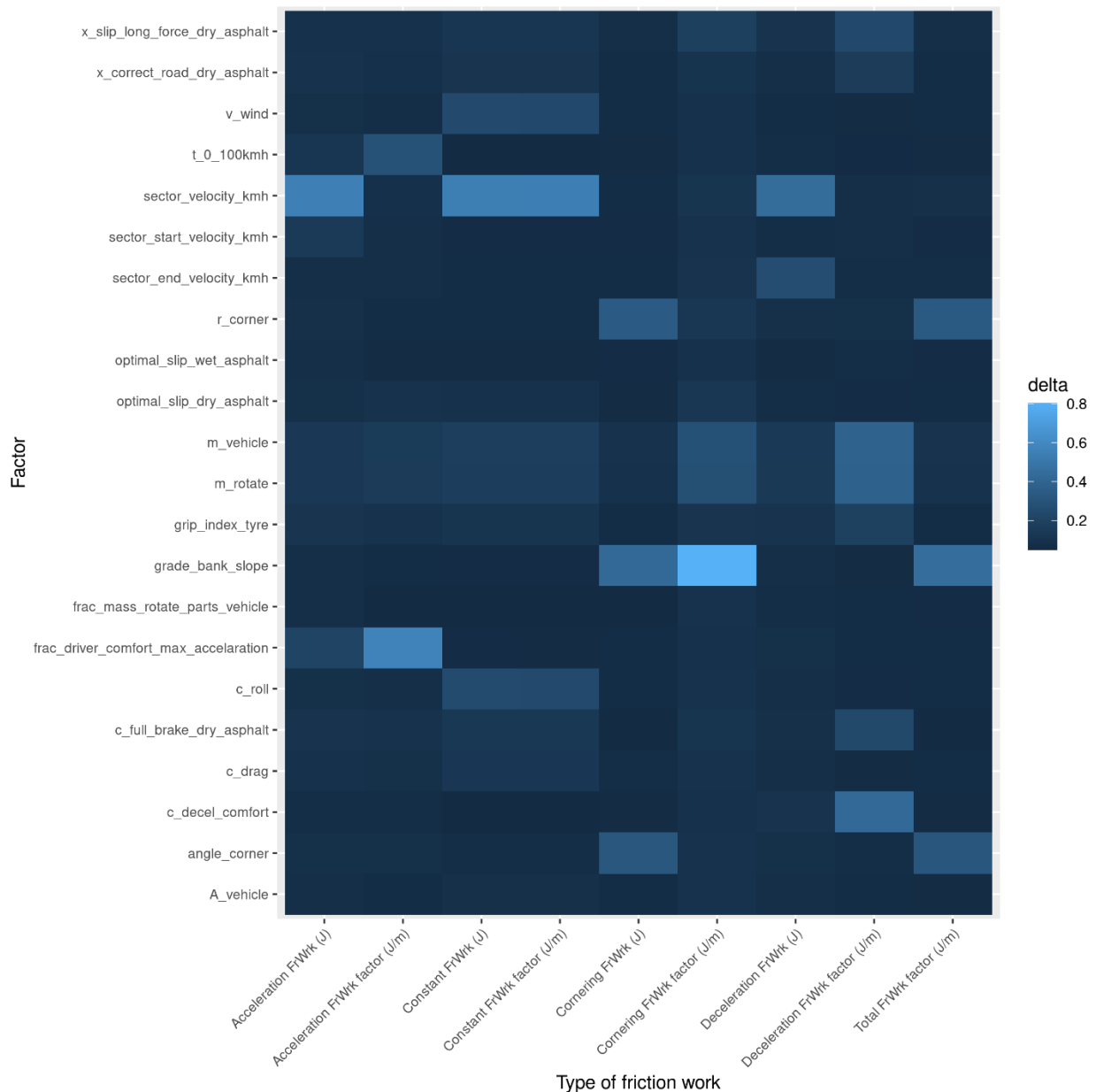


Figure 6: Sensitivity ranking of model parameters as described in Table 2, adapted to a flat road scenario (slope = 0%).

The most influential input parameter on the friction is the velocity of a vehicle (sector\_velocity\_kmh) when the influence of slope and bank slope are being discarded (Figure 7), which is logical.

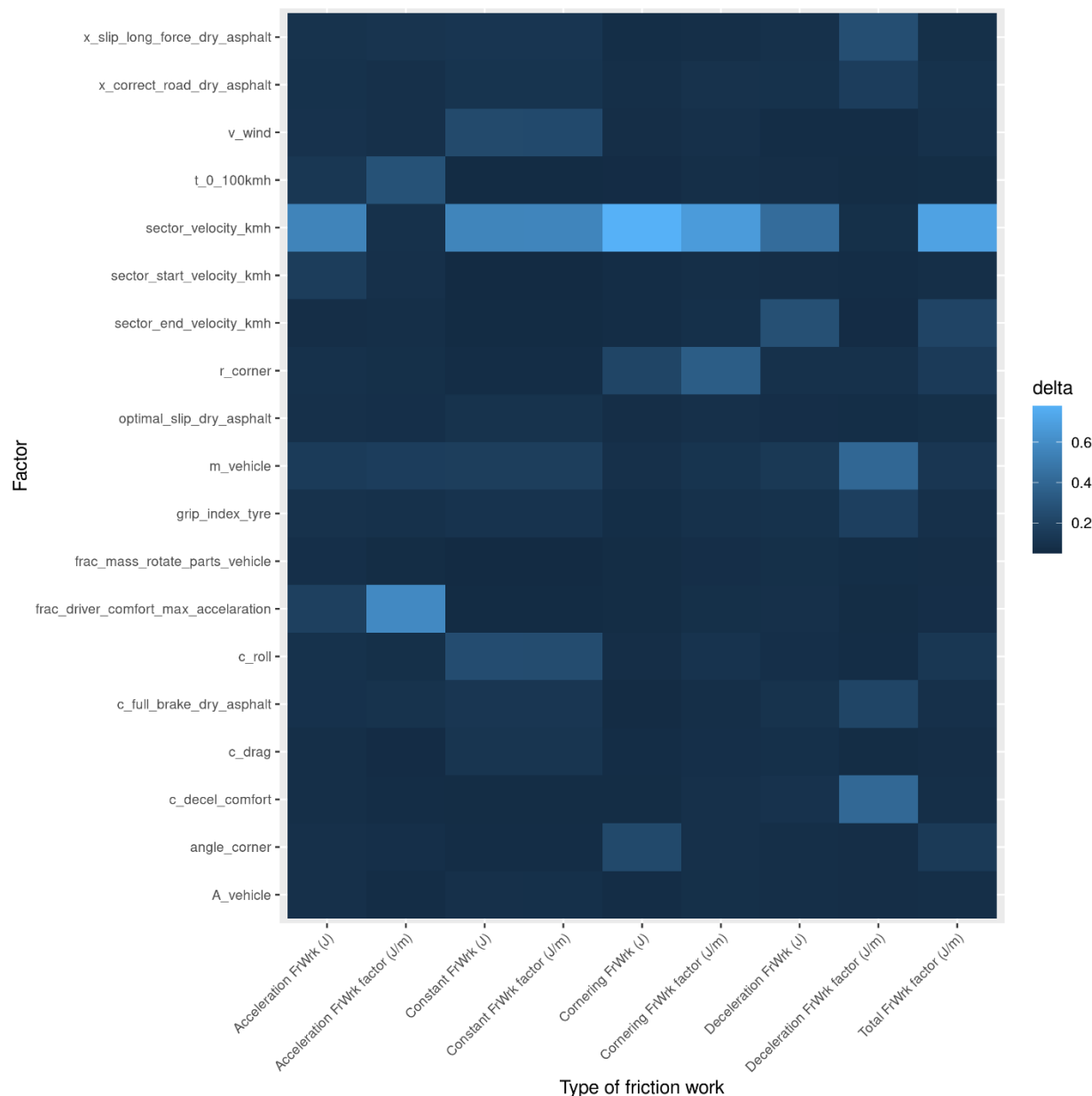


Figure 7: Sensitivity ranking of model parameters as described in Table 2, adapted to a no slope no bank slope scenario.

### 3.2 Estimated abrasion coefficients

The abrasion coefficient (n=25) is estimated based on the five sets of abrasion data for 5 tyre brands (Dunlop, Goodyear, Linglong, Michelin and Pirelli) representing rural, urban and motorway driving (Appendix II). The abrasion rates measured at the high intensity tests show an increasing wear rate for rural, motorway and urban scenarios (Figure 2a).

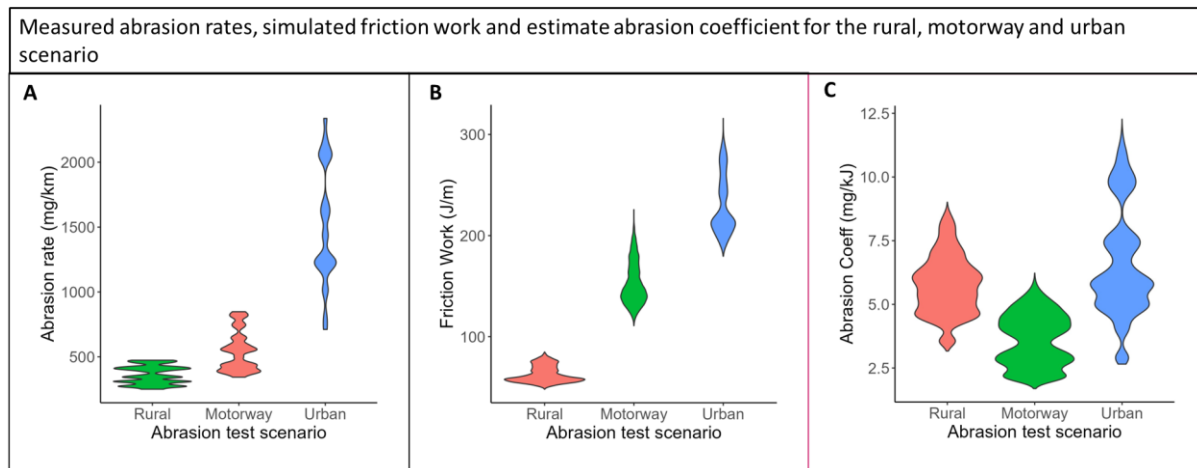


Figure 2. Violin plots of (A) measured tyre abrasion rates in mg/km (B) simulated friction work (J/m) and (C) estimated abrasion coefficients (mg/kJ) for the IDIADA test scenarios for rural, motorway and urban environments.

As expected the friction work calculations using the friction work model also show the same trend as the abrasion measurements, i.e. the friction work is the lowest for the rural scenario and highest for urban scenarios (Figure 2b). Dividing the measured abrasion rates (mg/km) with the respective simulated friction work per distance covered (J/m) for each scenario delivers estimated abrasion coefficients (mg/kJ) that are comparable within an order of magnitude (Figure 2C).

## 4 Discussion

### 4.1 Model evaluation

#### 4.1.1 Evaluation and validation of derived abrasion coefficients

Considering abrasion coefficient to be a tyre or material property is verified by the different scenarios with different intensity of performed vehicle maneuvers that nonetheless yield comparable abrasion coefficients (Figure 2A and 2C). The estimated abrasion coefficients ranging from 2 to 12.5 mg/kJ which is by order of magnitude comparable to abrasion coefficients reported in earlier tyre friction and abrasion investigations. Cenek et al. (1997) reported abrasion coefficients ranging from 1.8 to 11.2 mg/kJ derived from tyre abrasion measured with a so called GripTester, which is a device that keeps a wheel rolling over a road surface under controlled operating conditions such as constant wheel load, slip and speed. The aim of the investigations was to evaluate the abrasion of tyres at different road undergrounds, such as asphaltic concrete and slurry seal. i.e. a mixture of asphalt emulsion, crushed rock aggregates and other additives. As such, the abrasion coefficients derived from the data reported by Cenek et al.(1997) refer to the same type of tyre rolling over different undergrounds, whereas the IDIADA tyre wear measurements are performed with different tyre sets driving over the same track underground. Moreover,

Cenek et al. (1997) state that the ranges in the level of friction work performed on the tyre were too narrow (3.2 – 4.4 kJ/m) for sufficient evaluation of the impact of individual undergrounds on the tyre abrasion. Nonetheless, the overall ranges in abrasion coefficients reported by Cenek et al. (1997) are comparable to the overall ranges in abrasion coefficients estimated from the abrasion measurements performed at IDIADA and the modelled friction work based on the vehicle maneuvers in rural, motorway and urban scenarios.

The estimated abrasion coefficients (Figure 2C) are derived by dividing the measured abrasion rates (mg/km) with the simulated level of friction work performed per kilometre (J/km). The abrasion rates measured at the IDIADA tracks range from 250 to 474 mg/km for the rural scenario, 343 to 848 mg/km for the motorway scenario and 803 to 2338 mg/km for the urban scenario. As such, the range in estimated abrasion coefficient (2 to 12.5 mg/kJ) is also explained by the variability in the measured abrasion rates.

The abrasion rates at IDIADA are determined by an accelerated abrasion procedure characterized with a high driving severity number. The intensity of the maneuvers performed, e.g. high velocities at straight sectors and bends as well as strong accelerations and decelerations, are deliberately performed to yield relatively high tyre abrasion. IDIADA's measured abrasion rates are thus high compared to those presented in other tyre abrasion measurement data sources to characterize tyre wear at normal driving, such the tyre wear tests of ADAC (2021;2022; 2023; 2024) and the emission factors applied in national emission registration of tyre wear (Geilenkirchen et al., 2023). Typical emission factors used for instance in the Netherlands for estimating tyre wear from passenger cars are 132 mg per km driven in urban settings, 85 mg per km for rural settings and 104 mg per km for motorways. Hence, the abrasion rates measured for the rural scenario at IDIADA are a factor of 2.9 to 5.6 higher than the rural emission factors. The motorway scenario abrasion rates are a factor 3.3 to 8.2 larger than the national emission factor and for the urban scenario this is 6.1 to 17.7.

The friction and abrasion model results are still preliminary, because validation exercises by comparing the model outcomes with measurement on the field, track and indoor laboratory measurements are yet to be performed. Calibration exercises are desired as well as preliminary validation performed with abrasion measurements on the IDIADA track indicate slip during brake manoeuvre may be overestimated, whereas slip by wheelspin during constant speed driving and acceleration may be underestimated.

#### *4.1.2 More opportunities for model validation*

Abrasion measurement, TWP measurement in the field or track tests and abrasion measurements in indoor rollerbank experiments, are necessary to validate the tyre wear abrasion model use in estimating the release and emission of tyre wear. Indoor rollerbank measurements can provide abrasion coefficients for different sets of tyres that are measured under controlled indoor conditions. These abrasion coefficients can then be

inserted as input in model simulation runs to resemble the track tests in which a vehicle is driving over a circuit with known sector data and a controlled driving style. The simulated tyre abrasion should be comparable to the tyre abrasion measured at the track tests. If not, calibration of the model is needed. For instance, the percentage of slip as indicated should be verified with measurements and estimates of the friction force and slip of well characterised tracks and vehicle performance. Once the TWP emission model is calibrated it can be validated with actual measured concentrations of TWPs in the field at different types of areas, i.e rural roads, highway and urban streets for which the manoeuvre performed by the vehicles and the number of vehicles passing by are estimated.

#### *4.1.3 Calibration of peak friction coefficient and optimal slip*

The peak friction coefficient and optimal slip are important parameters in estimating the wheelspin (Figure 3), brake slip (Figure 4) and latitudinal slip. The peak friction coefficients are now estimated from correcting the peak friction coefficients given by the tyre grip index which refers to reference wet conditions at a reference asphalt track as described by the EC testing method procedure (EC, 2011). In case the validation exercises indicate the friction and abrasion model needs calibration, it would be the first step to evaluate the derivation of the peak friction coefficients and, if measurement data is available, replace them with actual peak friction coefficients measured at dry conditions on different types of underground. Such peak friction coefficients can be estimated from the brake way distance at a full wheellock brake manoeuvres. Furthermore, parameters influencing the friction between track and tyre and track, such as the texture, roughness or temperature of the road, are not directly included in the sensitivity analyses (section 3.1). Additional data describing friction coefficients between tyres and different undergrounds with different roughness, texture and temperature can be helpful to more accurately estimate the friction coefficient between a specific tyre and specific underground in order to further calibrate the friction and abrasion model.

#### *4.1.4 The importance of abrasion coefficient*

Abrasion coefficient is an important parameter in estimating the tyre wear abrasion due to the friction work performed on the tyre, but little to no data on abrasion coefficients are available in scientific literature (Fraunhofer et al., 2021; Gehrke et al., 2020). Current data on abrasion rates (mg/km) need abrasion coefficients to extrapolate the expected abrasion to different local landscapes and roads for which different vehicle manoeuvres are expected, e.g. speed limits, the level of traffic jams, an landscape slopes. As such, it is more effective to estimate or measure a tyre abrasion coefficient instead of measuring abrasion rates by (expensive) tests at different circumstances that are difficult to extrapolate to another, e.g. it is difficult to extrapolate abrasion rate measured on a flat

and straight highway sector to a mountain road which has with great variance in slope and many sharp and banked corners. Hence, accurate extrapolations of expected abrasion from one road to another requires data on abrasion coefficients.

## 4.2 Perspective

### *4.2.1 Adapting emission factors*

Current country derived emission factors are expressed in mg/km which were derived from abrasion rates of measurement performed in the past (Mennekes and Nowack, 2022). As such, the impact of innovations in vehicle and tyre design achieved in the last decades, such as the reduction of aerodynamic drag and roll resistance, are not included in the EFs. Once abrasion coefficients are derived, the TWP emission model that is based on the friction work performed on the tyres may be robust enough to replace the EFs.

### *4.2.2 Predicting impact of policy measures*

Near future policy measures may refer to increased tyre quality, driving style and future vehicle designs. The impact of such measures can be predicted with the TWP emission model by inserting values for the vehicle and tyre properties of the current vehicle population and driving conditions (e.g. speed limit) and performed another run with the desired vehicle design, tyre quality or driving conditions as desired by the policy measured. The TWP emission model can then deliver the amount of tyre wear reduced by one policy measure or a set of policy measures. The cost-effectivity of the policy measure can then be expressed by dividing the reduced tyre wear with the costs.

## 5 Conclusion

A proof of concept for an updated TWP emission model based on friction and abrasion has been presented. It appears that the abrasion coefficient can be an important Tyre related parameter for which more data is desired. One of the aims of this deliverable report was to demonstrate an approach to estimate such abrasion coefficients. This demonstration is given in section 3.2, but more precise data on the driving of the vehicle is needed. Abrasion measurement performed at different locations are desired as well in order to check whether abrasion at different tracks still yield similar abrasion coefficients. Once such robust data on abrasion coefficients is available, the model enables opportunities in reducing costs of track measurement, assessing cost-effectivity of policy measures and extrapolate TWP emissions (EFs) to different local landscapes and traffic situations. Model validation and calibration is however still necessary, but such exercises



are possible once measurement data is available from field, track, and indoor laboratory tests and experiments.

## 6 References

- AutoBild, 2021. Sommerreifen-Test 2023: Alle AUTO BILD-Tests in verschiedenen Größen [WWW Document]. URL <https://www.autobild.de/artikel/sommerreifen-test-5629291.html> (accessed 6.26.23).
- Borgonovo, E., 2007. A new uncertainty importance measure. *Reliability Engineering & System Safety* 92, 771–784. <https://doi.org/10.1016/j.ress.2006.04.015>
- Borrelle, S.B., Ringma, J., Law, K.L., Monnahan, C.C., Lebreton, L., McGivern, A., Murphy, E., Jambeck, J., Leonard, G.H., Hilleary, M.A., Eriksen, M., Possingham, H.P., De Frond, H., Gerber, L.R., Polidoro, B., Tahir, A., Bernard, M., Mallos, N., Barnes, M., Rochman, C.M., 2020. Predicted growth in plastic waste exceeds efforts to mitigate plastic pollution. *Science* 369, 1515–1518. <https://doi.org/10.1126/science.aba3656>
- Cenek, P.D., Carpenter, P., Jamieson, N.J., Stewart, P.F., 1997. Friction & tyre abrasion characteristics of New Zealand road surfaces, Transfund New Zealand research report. Transfund New Zealand, Wellington, N.Z.
- Cunha, R.H., da Silva, M.M., Costa Neto, Á., 2007. Modeling and qualitative analysis of tire wear for steady state cornering maneuvers, in: *Proceedings of the XII International Symposium on Dynamic Problems of Mechanics (DINAME 2007)*. Ilhabela, SP, Brazil.
- Da Silva, M.M., Cunha, R.H., Neto, A.C., 2012. A simplified model for evaluating tire wear during conceptual design. *Int.J Automot. Technol.* 13, 915–922. <https://doi.org/10.1007/s12239-012-0092-6>
- Directorate-General for Research and Innovation (European Commission), Groupe des conseillers scientifiques principaux, 2019. Environmental and health risks of microplastic pollution. Publications Office of the European Union, LU.
- EC, 2011. Commission Regulation (EU) No 228/2011 of 7 March 2011 amending Regulation (EC) No 1222/2009 of the European Parliament and of the Council with regard to the wet grip testing method for C1 tyres Text with EEA relevance.
- Ejsmont, J.A., Ronowski, G., Wilde, W.J., 2012. Rolling Resistance Measurements at the MnROAD Facility (Interim Report). Minnesota Department of Transportation.
- Ejsmont, J.A., Świczko-Żurek, B., Ronowski, G., Wilde, W.J., 2014. Rolling Resistance Measurements at the MnROAD Facility, Round 2 (Final Report). Minnesota Department of Transportation.
- EU, 2020. Regulation (EU) 2020/740 of the European Parliament and of the Council of 25 May 2020 on the labelling of tyres with respect to fuel efficiency and other parameters, amending Regulation (EU) 2017/1369 and repealing Regulation (EC) No 1222/2009 (Text with EEA relevance), OJ L.
- Fraunhofer, iMA, Sieker, 2021. Reifenabrieb – ein unterschätztes Umweltproblem? Digitales Planungs- und Entscheidungsinstrument zur Verteilung, Ausbreitung und Quantifizierung von Reifenabrieb in Deutschland (SCHLUSSBERICHT No. 19F2050A-C), TyreWearMapping.

- Gehrke, I., Dresen, B., Blomer, J., 2020. Modelling Of The Distribution Of Tyre Wear Particles in Germany. Presented at the 29th Aachen Colloquium Sustainable Mobility 2020.
- Geilenkirchen, G., Bolech, M., Hulskotte, J., Dellaert, S., Ligterink, N., Sijstermans, M., Geertjes, K., Felter, K., 't Hoen, M., 2023. Methods for calculating the emissions of transport in the Netherlands. PBL Netherlands Environmental Assessment Agency, The Hague.
- Grip, M., 2021. Tyre Performance Estimation during Normal Driving (Master of Science Thesis). Linköping University.
- Iooss, B., Veiga, S.D., Janon, A., Pujol, G., Broto, with contributions from B., Boumhaout, K., Delage, T., Amri, R.E., Fruth, J., Gilquin, L., Guillaume, J., Herin, M., Idrissi, M.I., Gratiet, L.L., Lemaitre, P., Marrel, A., Meynaoui, A., Nelson, B.L., Monari, F., Oomen, R., Rakovec, O., Ramos, B., Roustant, O., Sarazin, G., Song, E., Staum, J., Sueur, R., Touati, T., Verges, V., Weber, F., 2023. sensitivity: Global Sensitivity Analysis of Model Outputs.
- Kühlwein, J., 2016. Driving resistances of light-duty vehicles in Europe: present Situation, trends, and scenarios for 2025 (White Paper).
- Lau, W.W.Y., Shiran, Y., Bailey, R.M., Cook, E., Stuchtey, M.R., Koskella, J., Velis, C.A., Godfrey, L., Boucher, J., Murphy, M.B., Thompson, R.C., Jankowska, E., Castillo Castillo, A., Pilditch, T.D., Dixon, B., Koerselman, L., Kosior, E., Favoino, E., Gutberlet, J., Baulch, S., Atreya, M.E., Fischer, D., He, K.K., Petit, M.M., Sumaila, U.R., Neil, E., Bernhofen, M.V., Lawrence, K., Palardy, J.E., 2020. Evaluating scenarios toward zero plastic pollution. *Science* 369, 1455–1461. <https://doi.org/10.1126/science.aba9475>
- Mennekes, D., Nowack, B., 2022. Tire wear particle emissions: Measurement data where are you? *Sci Total Environ* 830, 154655. <https://doi.org/10.1016/j.scitotenv.2022.154655>
- Ntziachristos, L., Boulter, P., 2019. 1.A.3.b.vi-vii Road tyre and brake wear (No. Guidebook 2019), EMEP/EEA air pollutant emission inventory guidebook 2019. EMEP/EEA.
- Plischke, E., Borgonovo, E., 2020. Fighting the Curse of Sparsity: Probabilistic Sensitivity Measures From Cumulative Distribution Functions. *Risk Analysis* 40, 2639–2660. <https://doi.org/10.1111/risa.13571>
- Pohrt, R., 2019. TIRE WEAR PARTICLE HOT SPOTS – REVIEW OF INFLUENCING FACTORS. *FU Mech Eng* 17, 17. <https://doi.org/10.22190/FUME190104013P>
- R Core Team, 2023. R: A Language and Environment for Statistical Computing. R Foundation for Statistical Computing, Vienna, Austria.
- Schallamach, A., Turner, D.M., 1960. The wear of slipping wheels. *Wear* 3, 1–25. [https://doi.org/10.1016/0043-1648\(60\)90172-1](https://doi.org/10.1016/0043-1648(60)90172-1)
- Schwarz, A.E., Lensen, S.M.C., Langeveld, E., Parker, L.A., Urbanus, J.H., 2023. Plastics in the global environment assessed through material flow analysis, degradation and environmental transportation. *Science of The Total Environment* 875, 162644. <https://doi.org/10.1016/j.scitotenv.2023.162644>
- Steiner, M., 2020. Mikroplastik: Eintrag von Reifenabrieb in Oberflächengewässer. wst21, Bern.
- Verschoor, A.J., de Poorter, L.R.M., Roex, E., Bellert, B., 2014. Inventarisatie en prioritering van bronnen en emissies van microplastics [NL]. RIVM.

Zhang, Y., Kang, S., Allen, S., Allen, D., Gao, T., Sillanpää, M., 2020. Atmospheric microplastics: A review on current status and perspectives. *Earth-Science Reviews* 203. <https://doi.org/10.1016/j.earscirev.2020.103118>

## 7 Appendix I

### 7.1 Sensitivity analysis

#### 7.1.1 Additional sensitivity rankings

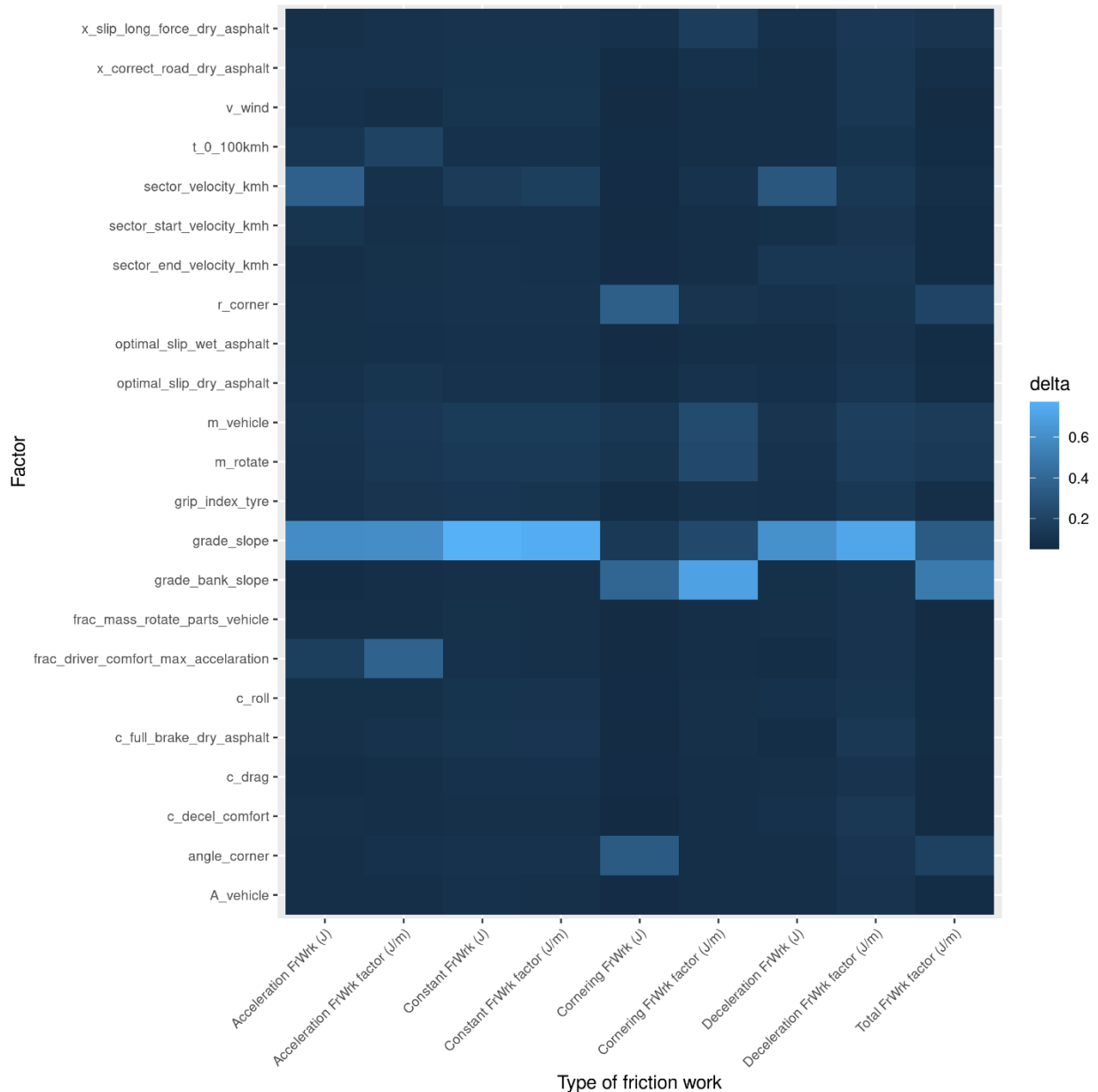


Figure 8: Sensitivity ranking of model parameters as described in Table 2, but with a 10 times lower slope (between -1 and 1 %).

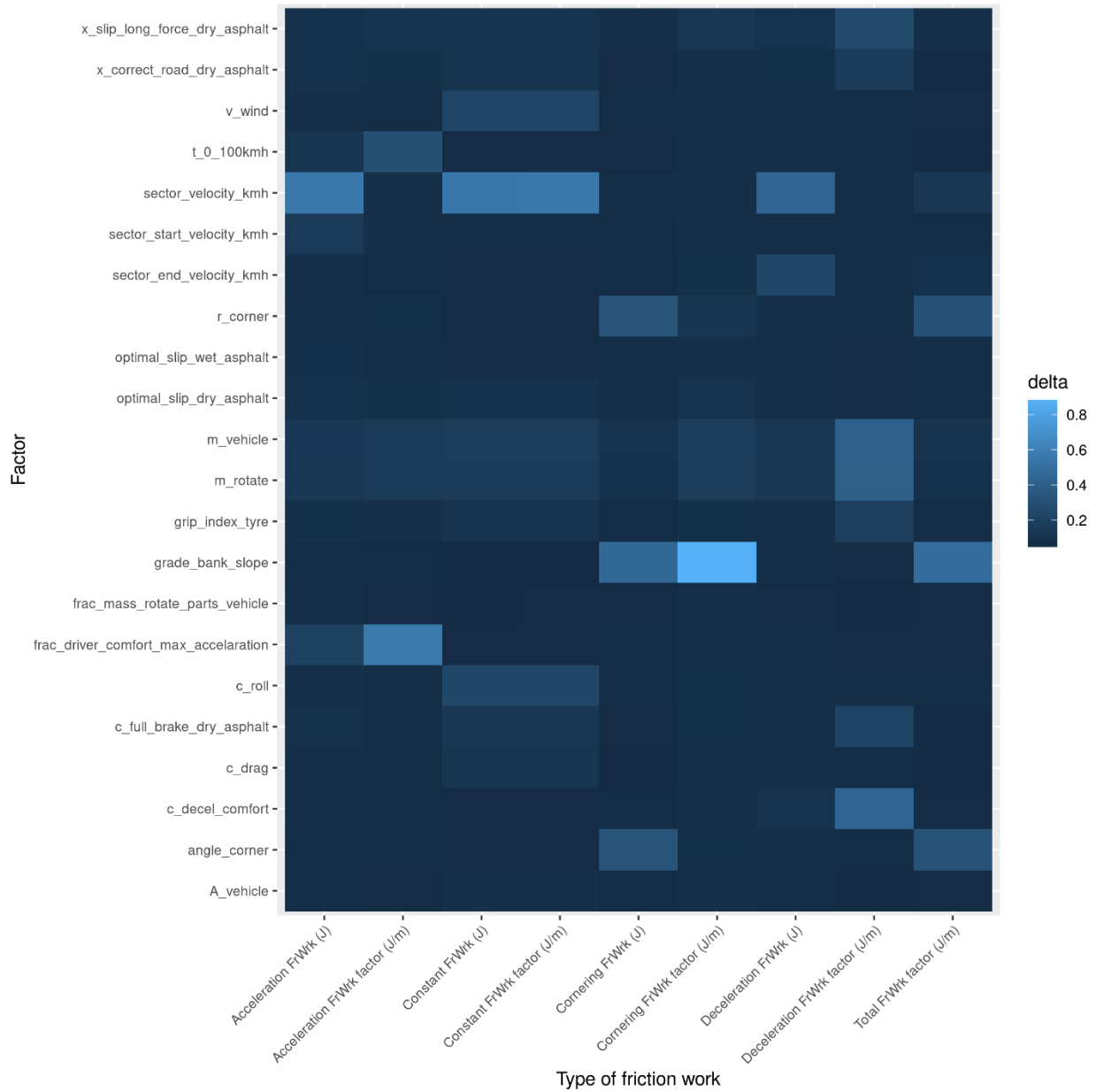


Figure 9: Sensitivity ranking of model parameters as described in Table 2, but for a flat road (Slope = 0) and a 10 times smaller bank slope (-1 to 1 %).

## 7.2 Tyre label data

Appendix 7.2 Table 1. Roll resistance coefficient (kg/t) ranges per fuel efficiency class according to EU 2020/740 quality tyre label.

	Roll resistance coefficient (kg/t)		
Label fuel efficiency class	Passenger cars (C1)	Light duty vehicles (C2)	Heavy duty vehicles (C3)
A	≤ 6.5	≤ 5.5	≤4.0
B	6.6 - 7.7	5.6 – 6.7	4.1 - 5.0
C	7.8 - 9.0	6.8 – 8.0	5.1 - 6.0
D	9.1 – 10.5	8.1 -9.0	6.1- 7.0-
E	≥ 10.6	≥9.1	≥7.1

Appendix 7.2 table 2. Table grip index ranges according to EU 2020/740

Label class	Wet grip index (G)		
Label wet grip class	Passenger cars (C1)	Light duty vehicles (C2)	Heavy duty vehicles (C3)
A	≥ 1.55	≥1.40	≥1.25
B	1.50 – 1.54	1.25 – 1.39	1.10 – 1.24
C	1.25-1.39	1.10 -1.24	0.95 – 1.09
D	1.10 – 1.24	0.95 – 1.09	0.80 – 0.94
E	≤ 1.09	≤0.94	≤0.79

## 8 Appendix II Circuit Run Data

### 8.1 Vehicle specifications

The model routines require the vehicle mass, aerodynamic drag coefficient, frontal area and mass of the rotating parts as input data. The circuit runs have been performed with a Ford Kuga Escape which a vehicle mass of 1660 kg and an aerodynamic drag coefficient of 0.347 and frontal area of 2.629 m<sup>2</sup>. The mass of the rotating part is estimated to be 216 to 249 kg which is 13 to 15% of the vehicle mass.

Appendix II Table 1 Vehicle specifications

Symbol	Description	Value	Unit
$A_{vehicle}$	Frontal area of vehicle	2.629	m <sup>2</sup>

$c_{drag}$	Aerodynamic drag coefficient	0.347	[-]
$m_{rotate}$	Mass of the rotating parts of the vehicle	216 – 249	kg
$m_{vehicle}$	Mass of the vehicle	1660	kg
$d_{vehicle}$	Vehicle turning diameter	11.7	m

## 8.2 Tyre quality and design

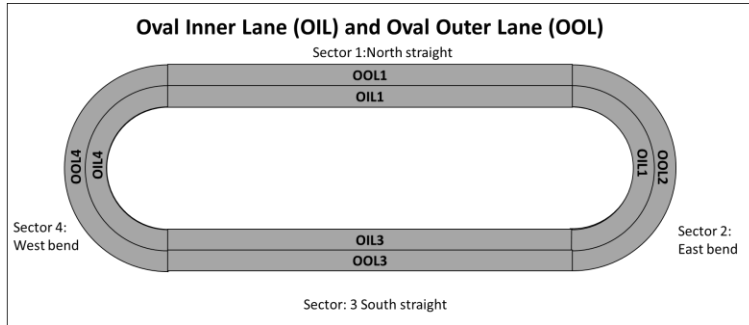
The model routines require the roll resistance coefficient (croll), brake force coefficient (cbrake.max) and the peak friction coefficient ( $\mu_{max}$ ) as input data expressing the interactions between tyre and track underground. In case such data is not directly available it is estimated from the EU Tyre Quality Labels for wet grip index and fuel consumption. Circuit runs have been performed for five sets of tyres (Appendix II Table 2)

Appendix II Table 2.

Tyre name	Wet grip index label	Grip index	Fuel consumption label	Roll resistance coefficient	Measured peak friction coefficient	Measured brake force coefficient
MICHELIN PILOT SPORT 4 SUV 225/60R18 100V	A	1.55 – 1.56	D	9.1 – 10.5		
GOODYEAR EFFICIENTGRIP SUV M+S 225/60R18 100V	B	1.40 – 1.54	C	7.9 – 9.0		
DUNLOP GRANDTREK ST30 M+S 225/60R18 100H	D	1.10 – 1.24	C	7.9 – 9.0		
PIRELLI SCORPION VERDE 225/60R18 100H	B	1.40 – 1.54	C	7.9 – 9.0		
LINGLONG BATMAN A50 SUV ATLAS M+S	C	1.25 -1.39	C	7.9 – 9.0		

## 8.3 IDIADA track and maneuver data

### 8.3.1 Oval track



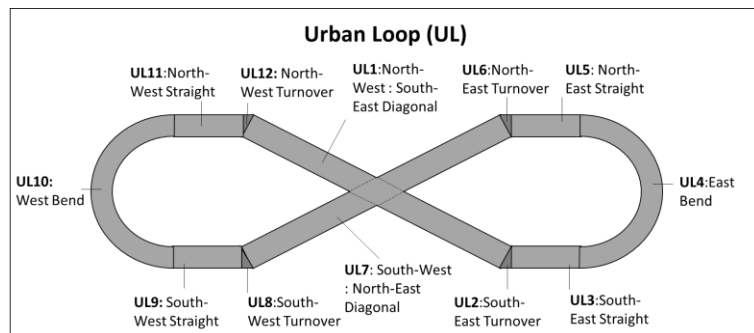
Appendix II Figure 1 Illustration of the IDIADA oval track

Appendix II Table .. Sector data of the IDIADA Oval Track

Sector number	Sector name	Sector distance (m)	Gradient slope (%)	Bank slope (%)		Corner radius (m)	Corner angle (degrees)
				Oval Inner Lane (OIL)	Oval Outer Lane (OOL)		
OIL 1/ OOL 1	North straight	1126	0	1	4	'Infinite'	0
OIL 1/ OOL 2	East bend	1477	0	1	4	470	180°
OIL 1/ OOL 3	South straight	1126	0	1	4	'Infinite'	0
OIL 1/ OOL 3	West Bend	1477	0	1	4	470	180°



### 8.3.2 Urban Loop



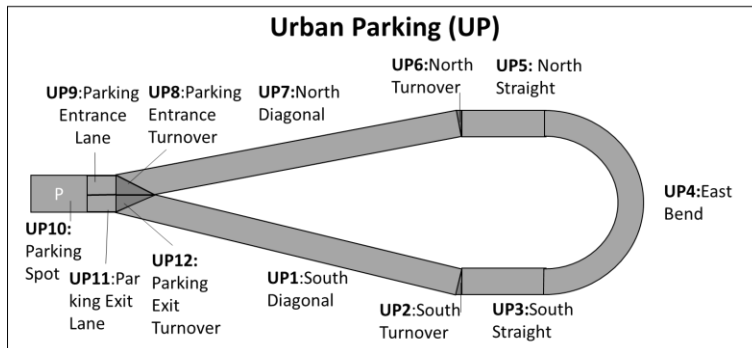
Appendix II Figure

Appendix II Table

Sector number	Sector name	Sector distance (m)	Gradient slope (%)	Bank slope (%)	Corner radius (m)	Corner angle (degrees)
UL1	North-West : South-East Diagonal	128	0	0	'Infinite'	0
UL2	South-East Turnover	3.6	0	0	½ vehicle turning diameter	35
UL3	South-East Straight	32	0	0	'Infinite'	0
UL4	East Bend	60	0	0	19.1	180
UL5	North-East Straight	32	0	0	'Infinite'	0
UL6	North-East Turnover	3.6	0	0	½ vehicle turning diameter	35
UL7	North-East : South-West Diagonal	128	0	0	'Infinite'	0
UL8	South-West Turnover	3.6	0	0	½ vehicle turning diameter	35
UL9	South-West Straight	32	0	0	'Infinite'	0
UL10	West Bend	60	0	0	19.1	180
UL11	North-West Straight	32	0	0	'Infinite'	0

UL12	North-West Turnover	3.6	0	0	½ vehicle turning diameter	35
------	------------------------	-----	---	---	-------------------------------------	----

### 8.3.3 Urban parking



Appendix II Figure

Appendix II Table

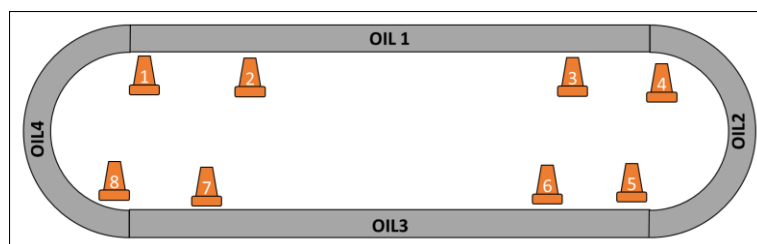
Sector number	Sector name	Sector distance (m)	Gradient slope (%)	Bank slope (%)	Corner radius (m)	Corner angle (degrees)
UP1	South Diagonal	331	0	0	'Infinite'	0
UP2	South Turnover	3.6	0	0	½ vehicle turning diameter	35
UP3	South Straight	32	0	0	'Infinite'	0
UP4	East bend	60	0	0	19.1	180
UP5	North Straight	32	0	0	'Infinite'	0
UP6	North Turnover	3.6	0	0	½ vehicle turning diameter	35
UP7	North Diagonal	331	0	0	'Infinite'	0
UP8	Parking entrance Turnover	3.6	0	0	½ vehicle turning diameter	35
UP9	Parking entrance lane	21	0	0	'Infinite'	0
UP10	Parking Spot	18.4	0	0	½ vehicle turning diameter	180
UP11	Parking Exit lane	21	0	0	'Infinite'	0
UP12	Parking Exit Turnover	3.6	0	0	½ vehicle turning diameter	35

## 8.4 Performed maneuvers

Vehicle maneuvers have been recorded and performed within eight different track runs representing a run-in procedure, rural driving, urban driving and motorways.

### 8.4.1 Run-in procedure

The objective of the run-in procedure was to eliminate the first part of the tire surface. A total distance of 1380 km has been covered during the run-in procedure divided over three days. Each day a distance of 460 km was driven followed by a weighing procedure. The run-in procedure was performed at the Oval Inner Lane (OIL) of the IDIADA track for which sector data is given in Appendix II Figure 1 and Appendix II table xx. There have been eight different vehicle maneuvers performed per lap during the run-in procedure for which maneuver data is presented in Appendix II figure 2 and Appendix II table ...



Appendix II Figure 2

Appendix II Table

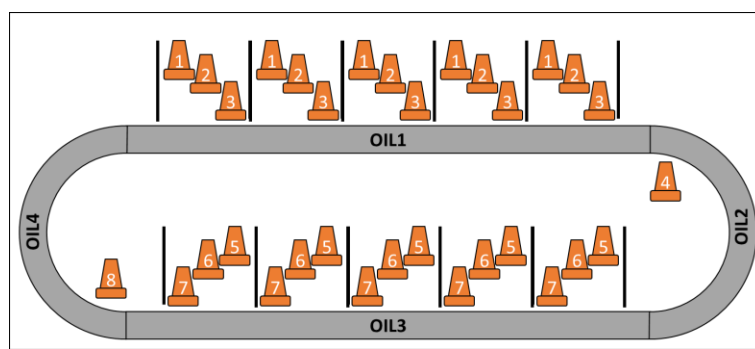
Maneuver number	Sector	Maneuver type	Start velocity (kph)	End velocity (kph)	Acceleration / decelation rate constant (m.s <sup>-2</sup> )
MRI1	OIL1	Acceleration	80	130	1.67
MRI2	OIL2	Constant speed	130	130	0
MRI3	OIL3	Deceleration	130	80	2.94
MRI4	OIL4	Constant speed	80	80	0
MRI5	OIL1	Acceleration	80	130	1.67
MRI6	OIL2	Constant speed	130	130	0
MRI7	OIL3	Deceleration	130	80	2.94
MRI8	OIL4	Constant speed	80	80	0

## 8.4.2 Rural driving

Three different rural driving scenarios have been driven as circuit runs at the oval inner lane (OIL) of the IDIADA Oval track ( Appendix II Figure 1).

### 8.4.2.1 Rural driving at 60 kph

The first rural driving scenario is driving 60 kph and brake to 50 kph and accelerate back to 60kph for five times at each straight sector of the IDIADA oval track. The bends are driven with 60 kph. A total number of 2 laps have been driven leading to a total distance of 15 km.



Appendix II Figure

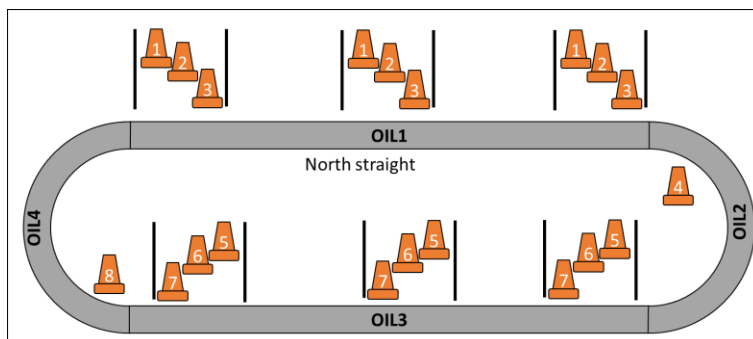
Maneuvers performed during the 60 kph rural driving scenario

Maneuver number	Sector	Maneuver type	Start velocity (kph)	End velocity (kph)	Acceleration / deceleration rate constant (m.s <sup>-2</sup> )	Maneuver repeats
MRu60kph1	OIL 1	Deceleration	60	50	1.0	5
MRu60kph2	OIL 1	Acceleration	50	60	1.0	5
MRu60kph3	OIL 1	Constant speed	60	60	0	5
MRu60kph4	OIL 2	Constant speed	60	60	0	1
MRu60kph5	OIL 3	Deceleration	60	50	1.0	5
MRu60kph6	OIL 3	Acceleration	50	60	1.0	5
MRu60kph7	OIL 3	Constant speed	60	60	0	5
MRu60kph8	OIL 4	Constant speed	60	60	0	1



### 8.4.2.2 Rural driving at 70 kph

The second rural driving scenario is driving 70 kph and brake to 50 kph and accelerate back to 70kph for three times at each straight sector of the IDIADA oval track. The bends are driven with 70 kph. A total number of 5 laps have been driven leading to a total distance of 37.1 km.



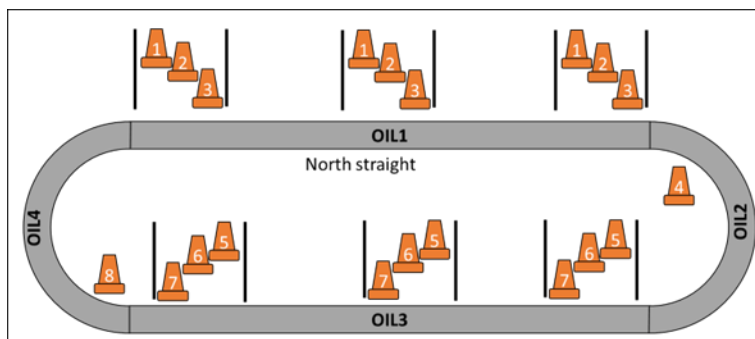
Appendix II Figure

Appendix II Table

Maneuver number	Sector	Maneuver type	Start velocity (kph)	End velocity (kph)	Acceleration / deceleration rate constant (m.s <sup>-2</sup> )	Maneuver repeats
MRu70kph1	OIL 1	Deceleration	70	50	1.4	3
MRu70kph2	OIL 1	Acceleration	50	70	1.4	3
MRu70kph3	OIL 1	Constant speed	70	70	0	3
MRu70kph4	OIL 2	Constant speed	70	70	0	1
MRu70kph5	OIL 3	Deceleration	70	50	1.4	3
MRu70kph6	OIL 3	Acceleration	50	70	1.4	3
MRu70kph7	OIL 3	Constant speed	70	70	0	3
MRu70kph8	OIL 4	Constant speed	70	70	0	1

### 8.4.2.3 Rural driving at 80 kph

The third rural driving scenario is driving 80 kph, brake to 50 kph and accelerate back to 80kph for three times at each straight sector of the IDIADA oval track. The bends are driven with 80 kph. A total number of 5 laps have been driven leading to a total distance of 37.1 km.



Appendix II Figure

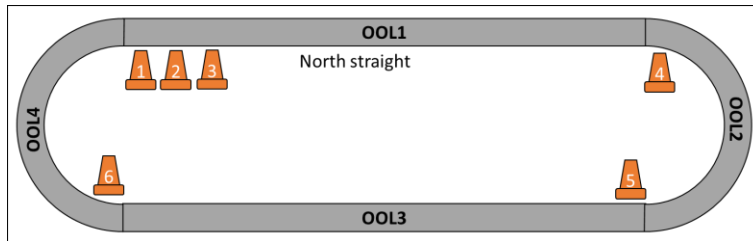
Appendix II Table

Maneuver number	Sector	Maneuver type	Start velocity (kph)	End velocity (kph)	Ac- /deceleration rate constant (m.s <sup>-2</sup> )	Maneuver repeats
MRu80kph1	OIL 1	Deceleration	80	50	2.94	3
MRu80kph2	OIL 1	Acceleration	50	80	1.6	3
MRu80kph3	OIL 1	Constant speed	80	80	0	3
MRu80kph4	OIL 2	Constant speed	80	80	0	1
MRu80kph5	OIL 3	Deceleration	80	50	2.94	3
MRu80kph6	OIL 3	Acceleration	50	80	1.6	3
MRu80kph7	OIL 3	Constant speed	80	80	0	3
MRu80kph8	OIL 4	Constant speed	80	80	0	1



### 8.4.3 Motorway

Motorway driving is represented with one scenario driven at the Oval Outer Lane (OOL) of the IDIADA tracks. The scenario includes a brake event in which a speed of 130 kph is decelerated to 50 kph followed by an acceleration event back to 130 kph at the north straight sector. The bends are driven at 130 kph. A total number of 15 laps have been driven leading to a total distance of 111 km.



Appendix II Figure

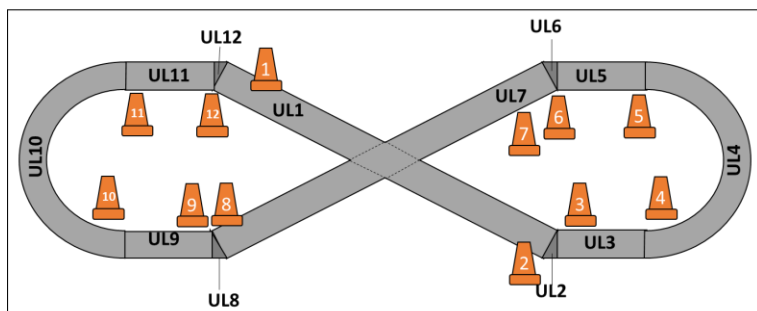
Appendix II Table

Maneuver number	Sector	Maneuver type	Start velocity (kph)	End velocity (kph)	Acceleration / deceleration rate constant (m.s <sup>-2</sup> )	Maneuver repeats
MMoW1	OOL 1	Deceleration	130	50	2.94	1
MMoW2	OOL 1	Acceleration	50	130	1.5	1
MMoW3	OOL 1	Constant speed	130	130	0	1
MMoW4	OOL 2	Constant speed	130	130	0	1
MMoW5	OOL 3	Constant speed	130	130	0	1
MMoW6	OOL 4	Constant speed	130	130	0	1

### 8.4.4 Urban driving

Urban driving have been evaluated by four scenarios. In the first scenario, the urban loop (UL) track at IDIADA has been driven with constant of 20kph. The second scenario is the same as the urban loop driving but with a brake event at one of the diagonal straight sectors (UL1). The third scenario is driven at the urban parking (UP) track at IDIADA and consists of driving 30 kph and a parking event. The fourth the scenario is also driven at the urban parking (UP) track at IDIADA and consists of driving 40 kph and a parking event.

#### 8.4.4.1 Urban loop constant speed driving at 20 kph



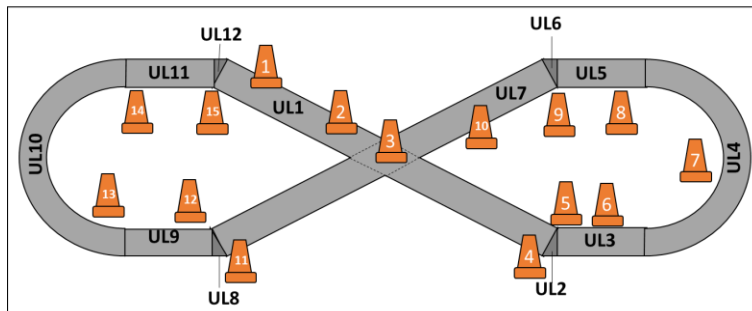
Appendix II Figure

Appendix II Table

Maneuver number	Sector	Maneuver type	Start velocity (kph)	End velocity (kph)	Acceleration / deceleration rate constant (m.s-2)	Maneuver repeats
MUcs20kph1	UL1	Constant speed	20	20	0	1
MUcs20kph2	UL2	Constant speed	20	20	0	1
MUcs20kph3	UL3	Constant speed	20	20	0	1
MUcs20kph4	UL4	Constant speed	20	20	0	1
MUcs20kph5	UL5	Constant speed	20	20	0	1
MUcs20kph6	UL6	Constant speed	20	20	0	1

MUcs20kph7	UL7	Constant speed	20	20	0	1
MUcs20kph8	UL8	Constant speed	20	20	0	1
MUcs20kph9	UL9	Constant speed	20	20	0	1
MUcs20kph10	UL10	Constant speed	20	20	0	1
MUcs20kph11	UL11	Constant speed	20	20	0	1
MUcs20kph12	UL12	Constant speed	20	20	0	1

### 8.4.4.2 Urban loop driving at 20 kph with brake event



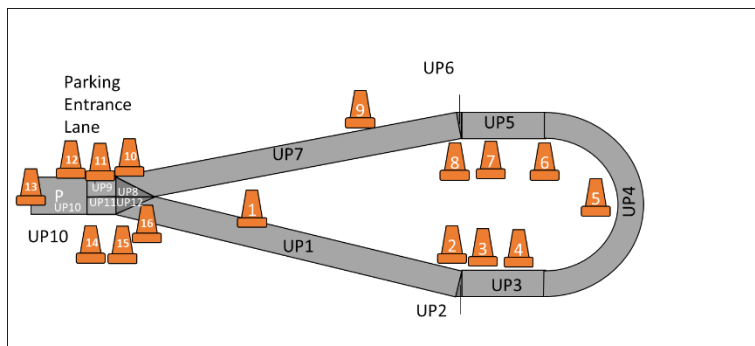
Appendix II Figure

Appendix II Table

Maneuver number	Sector	Maneuver type	Start velocity (kph)	End velocity (kph)	Acceleration / deceleration rate constant (m.s-2)	Maneuver repeats
MUbr20kph1	UL1	Deceleration	20	0	1.11	1
MUbr20kph2	UL1	Acceleration	0	20	1.11	1
MUbr20kph3	UL1	Constant speed	20	20	0	1
MUbr20kph4	UL2	Constant speed	20	20	0	1
MUbr20kph5	UL3	Constant speed	20	20	0	1
MUbr20kph6	UL4	Constant speed	20	20	0	1
MUbr20kph7	UL5	Constant speed	20	20	0	1
MUbr20kph8	UL6	Constant speed	20	20	0	1
MUbr20kph9	UL7	Constant speed	20	20	0	1
MUbr20kph10	UL8	Constant speed	20	20	0	1
MUbr20kph11	UL9	Constant speed	20	20	0	1

MUbr20kph12	UL10	Constant speed	20	20	0	1
MUbr20kph13	UL11	Constant speed	20	20	0	1
MUbr20kph14	UL12	Constant speed	20	20	0	1

### 8.4.4.3 Urban driving at 20 and 30 kph with parking event



Appendix II Figure

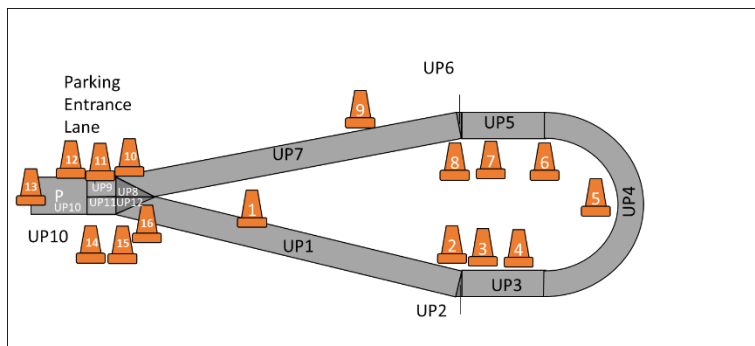
Appendix II Table

Maneuver number	Sector	Maneuver type	Start velocity (kph)	End velocity (kph)	Acceleration / deceleration rate constant (m.s-2)	Maneuver repeats
MUpa30kph1	UP 1	Constant speed	30	30	0	1
MUpa30kph2	UP 2	Constant speed	30	30	0	1
MUpa30kph3	UP 3	Deceleration	30	20	2.94	1
MUpa30kph4	UP 3	Constant speed	20	20	0	1
MUpa30kph5	UP 4	Constant speed	20	20	0	1
MUpa30kph6	UP 5	Acceleration	20	30	1	1
MUpa30kph7	UP 5	Constant speed	30	30	0	1
MUpa30kph8	UP 6	Constant speed	30	30	0	1
MUpa30kph9	UP7	Constant speed	30	30	0	1
MUpa30kph10	UP8	Constant speed	30	30	0	1
MUpa30kph11	UP 9	Constant speed	30	30	0	1
MUpa30kph12	UP 9	Deceleration	30	0	2.94	1

MUpa30kph12	Up 10	Acceleration	0	21.8 A	1	1
MUpa30kph13	UP11	Acceleration	21.8 A	30	1	1
MUpa30kph14	UP11	Constant Speed	30	30	1	1
MUpa30kph15	UP12	Constant Speed	30	30	1	1

A: calculated as  $\sqrt{c_{accel}2S}$

### 8.4.4.4 Urban driving at 20 and 40 kph with parking event



Appendix II Figure

Appendix II Table

Maneuver number	Sector	Maneuver type	Start velocity (kph)	End velocity (kph)	Acceleration / deceleration rate constant (m.s <sup>-2</sup> )	Maneuver repeats
1	South Diagonal	Constant speed	40	40	0	1
2	South Turnover	Constant speed	40	40	0	1
3	South Straight	Deceleration	40	20	2.94	1
4	South Straight	Constant speed	20	20	0	1
5	East Bend	Constant speed	20	20	0	1
6	North Straight	Acceleration	20	40	1	1
7	North Straight	Constant speed	40	40	0	1
8	North Turnover	Constant speed	40	40	0	1
9	North Diagonal	Constant speed	40	40	0	1
10	Parking Entrance Turnover	Constant speed	40	40	0	1
11	Parking Entrance Lance	Deceleration	40	0	2.94	1



12	Parking Spot	Acceleration	0	21.8 <sub>A</sub>	1	1
13	Parking Exit Lane	Acceleration	21.8 <sup>A</sup>	40	1	1
14	Parking Exit Lane	Constant Speed	40	40	1	1
15	Parking Exit Turnover	Constant Speed	40	40	1	1

A: calculated as  $\sqrt{c_{accel}2S}$